Atmos. Meas. Tech. Discuss., 3, 1707–1742, 2010
www.atmos-meas-tech-discuss.net/3/1707/2010/

Atmospheric Measurement Techniques Discussions

This discussion paper is/has been under review for the journal Atmospheric Measurement Techniques (AMT). Please refer to the corresponding final paper in AMT if available.

Impact of temperature field inhomogeneities on the retrieval of atmospheric species from MIPAS IR limb emission spectra

M. Kiefer[1], E. Arnone[2], A. Dudhia[3], M. Carlotti[2], E. Castelli[4], T. von Clarmann[1], B. M. Dinelli[4], A. Kleinert[1], A. Linden[1], M. Milz[1,*], E. Papandrea[2], and G. Stiller[1]

[1]Karlsruhe Institute of Technology, Institute for Meteorology and Climate Research, Karlsruhe, Germany
[2]Dip. to di Chimica Fisica e Inorganica, Universitá di Bologna, Italy
[3]University of Oxford, AOPP, Oxford, UK
[4]ISAC-CNR – Istituto di Scienze dell'Atmosfera e del Clima – CNR, Bologna, Italy
[*]now at: Department of Space Science, Luleå University of Technology, Kiruna, Sweden

Received: 22 March 2010 – Accepted: 6 April 2010 – Published: 14 April 2010

Correspondence to: M. Kiefer (michael.kiefer@kit.edu)

Published by Copernicus Publications on behalf of the European Geosciences Union.

Abstract

We examine volume mixing ratios (vmr) retrieved from limb emission spectra recorded with the Michelson Interferometer for Passive Atmospheric Sounding (MIPAS). In level 2 (L2) data products of three different retrieval processors, which perform one dimensional (1-D) retrievals, we find significant differences between species' profiles from ascending and descending orbit parts. The relative differences vary systematically with time of the year, latitude, and altitude. In the lower stratosphere their monthly means can reach maxima of 20% for CFC-11, CFC-12, HNO_3, H_2O, 10% for CH_4 and N_2O. Relative differences between monthly means of 1-D retrieval results and of the true atmospheric state can be expected to reach half of these percentage values, while relative differences in single vmr profiles might well exceed those numbers. Often there are no physical or chemical reasons for these differences, so they are an indicator for a problem in the data processing. The differences are generally largest at locations where the meridional temperature gradient of the atmosphere is strong. On the contrary, when performing the retrieval with a tomographic two dimensional (2-D) retrieval, L2 products generally do not show these differences. This implies that inhomogeneities in the temperature field, and possibly in the species' fields, which are accounted for in the 2-D algorithm and not in standard 1-D processors, may cause significant deviations in the results. Inclusion of an externally given adequate temperature gradient in the forward model of a 1-D processor helps to reduce the observed differences. However, only the full tomographic approach is suitable to resolve the horizontal inhomogeneities. Implications for the use of the 1-D data, e.g. for validation, are discussed. The dependence of the ascending/descending differences on the observation strategy suggests that this problem is to be expected to affect in general 1-D retrievals of infrared limb sounders, if the line of sight of the instrument has a significant component in the direction of the horizontal temperature variation.

AMTD

3, 1707–1742, 2010

1 Introduction

1.1 MIPAS on Envisat

MIPAS, the Michelson Interferometer for Passive Atmospheric Sounding, is a mid-infrared emission Fourier transform spectrometer which is part of the core payload of Envisat (Fischer et al., 2000, 2008). It scans the atmosphere vertically in limb geometry detecting atmospheric thermal radiation from the middle atmosphere and upper troposphere. The instrument shares in the advantages common to IR limb emission sounders, namely a) good sensitivity due to collecting photons along a long line of sight (LOS), b) good vertical resolution, since the majority of the signal is emitted close to the tangent point, c) independence on external radiation sources, which means that measurements during day and night, especially important at polar night, can be performed.

MIPAS is installed at the rear of Envisat. In its nominal observation mode it is looking backwards with respect to the satellite's flight direction. Envisat performs a sun-synchronous near polar orbit at 800 km altitude (14.4 orbits per day) with the descending node crossing at 10:00 MST (mean solar time). Because of the associated longitude drift of the orbit MIPAS measures limb radiance spectra of a certain region on Earth with approximately 12 h difference with the dayside data being measured during the descending and the nightside data during the ascending part of the orbit.

1.2 Motivation

Several scientific algorithms have been developed to retrieve the concentration of atmospheric species from MIPAS spectra. Among a number of common assumptions, the so called one dimensional (1-D) algorithms assume a horizontally homogeneous atmosphere along the LOS since the largest variations in the atmosphere occur in the vertical direction. On the contrary, the tomographic 2-D retrieval by Carlotti et al. (2001) was developed to model the horizontal gradients as seen by MIPAS LOS since, espe-

AMTD
3, 1707–1742, 2010

cially in regions of strong gradients, the assumption of homogeneity along the LOS can fail.

Although e.g. Livesey and Read (2000) for Aura/MLS and Carlotti et al. (2001, 2006) and Steck et al. (2005) for MIPAS discussed the advantages of being able to model the inhomogeneity of the atmospheric fields, no systematic assessment of shortages in 1-D results due to the horizontal homogeneity assumption was performed up to now.

A first hint that there are differences in MIPAS 1-D retrieval results depending on what appeared to be due to day/night conditions was discovered by Höpfner et al. (2007). In that work several species retrieved with the IMK/IAA L2 processor were compared to results of ACE-FTS (Bernath, 1999; Bernath et al., 2005) measurements. A separation of data with respect to several criteria was performed to check for in/out vortex and day/night conditions. Notably in CFC-11 there was a clear influence of whether day or night data of IMK/IAA was chosen (see Figs. 6 and 7 of Höpfner et al. (2007)). MIPAS daytime values were by about 10% higher than their nighttime counterparts. CFC-12 also showed a day/night difference, albeit with a magnitude of 5–10% somewhat less pronounced (see Fig. 8 ibid.). Since ACE data was not separated accordingly (there is occultation data for sunrise and sunset data, but only the latter one had been used for the comparison) but rather remained unchanged, the conclusion was that there is an anomaly in the version of MIPAS CFC-11 and CFC-12 data adopted for the comparison. In subsequent investigations this anomaly was associated with shortages in the 1-D retrieval of MIPAS data, depending on whether vmr profiles were retrieved for ascending or descending orbit parts, and on the different horizontal temperature gradients crossed by the instrument lines of sight.

These shortages, together with the different assumption adopted by 1-D and 2-D retrievals, motivates the thorough analysis of the impact of temperature inhomogeneity on the retrieved results presented in this paper.

2 Processing of MIPAS data

2.1 Level 1b processing

The level 1b (L1b) processing, i.e. the generation of geolocated and radiometrically calibrated near IR limb radiance spectra from the instrument's detectors output is done exclusively by ESA. A detailed description of the procedure can be found in Kleinert et al. (2007). All of the level 2 processors described in the following use the L1b data of this same source.

2.2 L2 processing

L2 data, i.e. the geolocated atmospheric physical and chemical quantities derived from L1b spectra, are estimated by fitting synthetic spectra produced with radiative transfer models to the observations. In this work we consider 1-D and 2-D retrievals of MIPAS data. Here the term 1-D retrieval is used for retrievals where, based on the fact that the bulk of information comes from the region close to the tangent height, the atmosphere is assumed to be horizontally homogeneous with respect to mixing ratios of constituents and to temperature and pressure. On the contrary in 2-D retrievals the atmospheric state is allowed to vary also in the horizontal (Carlotti et al., 2001; Steck et al., 2005). The assumption of horizontal homogeneity fails in presence of e.g. strong horizontal gradients, which are modelled in the 2-D approach by a simultaneous fit of the complete orbit.

A common feature of all 1-D processors considered here and the 2-D processor is that only small parts of the measured spectrum, so-called microwindows, which depend on retrieval target and altitude are used (von Clarmann and Echle, 1998; Dudhia et al., 2002). The spectral positions and extents of the microwindows might differ between the diverse processors, depending on the retrieval target. Some details of the adopted 1-D and 2-D retrievals are briefly summarized hereafter.

AMTD
3, 1707–1742, 2010

2.3 1-D retrievals

In this paper we present data of three different 1-D MIPAS L2 retrieval processors, namely the ESA offline processor (data designated ESA), the University of Oxford MORSE/OPTIMO processor (data designated Oxford), and the IMK/IAA processor(designation IMK/IAA). Apart from the use of microwindows the 1-D processors have in common some more properties:

- The retrieval is performed with global fit approach (Carlotti, 1988).
- The retrieval sequence starts with joint retrieval of temperature and an altitude coordinate, which is tangent pressure for ESA and Oxford processors, and tangent altitude for the IMK/IAA processor.
- The retrieval targets are processed sequentially (some exceptions are discussed below).

It has to be noted that any error in the result of the first processing step, i.e. the retrieval of the temperature profile, will propagate into the species profiles' retrievals.

2.3.1 ESA Offline L2 processor

A thorough description of this processor is given by Raspollini et al. (2006).

2.3.2 Oxford University L2 processor

The Oxford L2 processor, MORSE (MIPAS Orbital Retrievals using Sequential Estimation, documentation at http://www.atm.ox.ac.uk/MORSE/) mainly differs from the ESA processor in using optimal estimation (Rodgers, 2000) rather than a regularized least squares fit approach. The optimal estimation provides certain advantages in numerical stability, at the risk of introducing a bias, and the sequential aspect allows memory

AMTD
3, 1707–1742, 2010

usage to be minimised (at the expense of increased CPU time), effectively by incorporating measurements from just one microwindow/tangent altitude at a time rather than all simultaneously.

It uses the same microwindows and absorption coefficient look-up tables as the ESA processor for the main target species, and additionally retrieves CFC-11, CFC-12, N_2O_5 and $ClONO_2$.

The internal forward model is based on the RFM (Reference Forward Model, http://www.atm.ox.ac.uk/RFM) but using the pretabulated monochromatic absorption coefficients rather than a full line-by-line calculation.

The a priori estimates required for the optimal estimation approach are taken from the climatology of Remedios et al. (2007) (which also provides the initial guess for the ESA retrievals). These do not distinguish between day and night or longitude, so the a priori estimates used at a particular latitude are identical for the ascending and descending passes within any one day.

2.3.3 IMK/IAA Scientific L2 processor

The retrieval strategy employed in the IMK/IAA L2 processor has been extensively discussed by von Clarmann et al. (2003). The regularization of the least squares fit is a Tikhonov-type first-order smoothing constraint for temperature and volume mixing ratios. Multiple target retrievals are performed whenever necessary to avoid propagation of errors due to uncertain parameters.

For the bulk of IMK/IAA data presented here, the atmosphere is assumed to be horizontally homogeneous with respect to mixing ratios of constituents and temperature. Data of data versions V3O_T_8 (as input for species' retrievals), V3O_F-11_8 and V3O_HNO3_7 presented here were retrieved with the 1-D version of the IMK/IAA processor. However, the L2 processor is capable of taking into account some properties of a horizontally inhomogeneous atmosphere, e.g. the inclusion of externally given gradients of temperature and/or species, together with a proper length scale, in the forward model. A more sophisticated method, namely the retrieval of temperature gradients,

constrained by a priori information from ECMWF data, is routinely used for more recent IMK/IAA retrievals, e.g. for the L2 data of reduced resolution spectra for MIPAS data from 2005 on (von Clarmann et al., 2009). The retrieval of horizontal vmr gradients is routinely employed in the L2 processing of NO, NO_2, and CO (Funke et al., 2009).

2.4 2-D retrieval

Two-dimensional retrievals have been operated with the GMTR analysis system fully described in Carlotti et al. (2006). GMTR was developed as an open source code, specifically designed for MIPAS measurements, delivered to ESA and included in the BEAT tools repository (http://envisat.esa.int/services/beat). The upgraded version 2.1 of GMTR was used to generate the MIPAS2-D database of level 2 products used in this paper (Papandrea et al., 2010; Dinelli et al., 2010).

Version 2.1 of GMTR can be exploited for the analysis of all the MIPAS configurations and includes the possibility of performing retrievals using the Optimal Estimation method (Rodgers, 2000). This new functionality was introduced to better handle measurements affected by clouds in the line of sight, and to cope with the limb-scanning pattern that changes with latitude.

The GMTR analysis system is based on the Geo-fit approach (Carlotti et al., 2001) upgraded with the Multi-Target Retrieval (MTR) functionality (Dinelli et al., 2004).

With the Geo-fit MIPAS observations taken along the orbit track are analyzed in two dimensions by exploiting the fact that the limb sequences are continuously repeated along the plane of the orbit. This repetition makes it possible to gather the information about a given location of the atmosphere from all the lines of sight that cross that location whatever sequence they belong to. Since the loop of overlap between nearby sequences closes when the starting sequence is reached again at the end of the orbit, in a retrieval analysis the full gathering of information can be obtained by merging in a simultaneous fit the observations of a complete orbit. The Geo-fit approach operates a 2-D discretization of the atmosphere which enables to model horizontal atmospheric inhomogeneities. A remarkable feature of Geo-fit is that the retrieval grid is independent

AMTD
3, 1707–1742, 2010

of the measurement grid so that atmospheric profiles can be retrieved with horizontal separations different from those of the measured limb scans. This feature makes it possible to define the horizontal resolution of the retrieval on the basis of its trade-off with the precision of the retrieval parameters (Carlotti et al., 2007).

The MTR approach enables to perform simultaneous retrievals of different targets that can interfere, thus eliminating the systematic error components due to the propagation of the uncertainties on pressure, temperature and on the concentrations of the molecules included in the fit that could affect the retrieved targets.

The data of GMTR will be designated MIPAS2D in what follows.

3 Survey of the anomaly

To explore the problem broached in Sect. 1.2 we examined retrieval results of a time span from the beginning of the mission in mid 2002 to the temporary break in March 2004 of several 1-D L2 processors (ESA, Oxford, and IMK/IAA) and 2-D results (Bologna) for several species.

3.1 Analysis method

For each of the 1-D processors and for the 2-D processor the data was treated in the following manner: first, all vertical profiles of volume mixing ratios were interpolated onto a fixed reference pressure grid, having the equivalent of a 1 km vertical step in log-pressure. Then the whole data set was separated into data of geolocations of ascending and of descending orbit parts. In the next step each of these ascending/descending subsets was sorted into time bins of 30.4369 days (representing the length of a mean month) and latitude bins of 15°. Finally mean profiles within the time/latitude bins were calculated. Hence for each bin there are two mean profiles: one calculated from profiles of the ascending and one calculated from profiles of the descending part of the orbit.

In the following we present mean profiles, which are calculated as mean of ascending and descending profiles, difference profiles, which represent the differences of the means between ascending and descending data (i.e. ascending minus descending), and relative differences, which are the latter divided by the former. Atmospheric pressure is used as the altitude coordinate throughout the study.

We concentrate mostly on the latitude band from 65° S to 45° S where the anomaly can be seen very clearly. We shall use negative/positive signs of latitudes synonymous to S/N indicators for southern/northern latitudes.

3.2 Results for key species

We present here the analysis of ascending/descending differences for a number of key species retrieved from MIPAS spectra, which all have a fundamental role as greenhouse effect and/or ozone chemistry. The analysis focuses on gases having different distribution, so as to cover the typically observed scenarios of atmospheric gradients. In particular, CFC-11 originally discussed by Höpfner et al. (2007) is taken as an example of gas of tropospheric origin, HNO_3 for gases with strong local production in the stratosphere. Water vapour is discussed separately for its peculiar distribution. CH_4, N_2O and CFC-12 are briefly reported to show the level of consistency among these relevant gases.

In the following, each species is discussed adopting specific 1-D retrieval algorithms which most clearly depict the anomalous behaviour or have the best time coverage. Unless specific comments are made, results from the different 1-D retrievals are consistent in terms of the main altitude/latitude/time features of the anomaly.

3.2.1 CFC-11

The first case we analyse is CFC-11, a gas once released in the troposphere, showing a height independent vmr in the troposphere, and stratospheric gradients which are negative with latitude and altitude.

Figure 1 features pressure versus time plots for the latitude bin 60° S–45° S. The differences in 1-D data (first two rows, second and third panel from the left) show a pronounced annual cycle with higher CFC-11 in profiles of ascending orbit parts during northern summer and lower values during northern winter with a similar time behaviour among the 1-D processors. Peak values are reached at 70–100 hPa for IMK/IAA and 100–200 hPa for Oxford data. In general the most pronounced differences for Oxford data are located mostly in the region where the CFC-11 profile still is almost constant or has a weak vertical gradient, while the IMK/IAA's CFC-11 differences are mostly found in the region of the greatest vertical CFC-11 gradient. This might be caused by the different methods of constraining the retrieval, see Sects. 2.3.2 and 2.3.3. Both datasets exhibit maximum relative differences of more than ±20% below 70 hPa (the pressure level at which CFC-11 has decreased to approximately half of the ground/maximum value). Large relative differences above 20–30 hPa are due to low absolute values of CFC-11 at these altitudes.

MIPAS2-D data do not show a clear pattern below 40 hPa neither in absolute nor in relative differences. The differences rather are close to zero or do exhibit a seemingly random pattern above 80 hPa. Only relative differences at pressure levels around 30 hPa depict an annual cycle with amplitude comparable to that of 1-D data, while the phase is shifted by 1/2 year although at a magnitude comparable to measurement uncertainties.

In Fig. 2 Oxford and MIPAS2-D data are displayed in latitude versus time plots at 80 hPa and 82 hPa, respectively. In both hemispheres, the sign of the differences in 1-D data essentially is the same for all latitudes for a given time. However, the sign changes in the course of the year, but not with local season. Ascending data exhibits greater vmr values than descending data around JJA-months and smaller values around DJF-months. At this pressure level the major differences are located in the Southern Hemisphere in a band from 75° S–30° S. In the Northern Hemisphere the amplitude of the annual variation is weaker than in the south. CFC-11 of IMK/IAA (not shown in the Figure) exhibits a very similar pattern, albeit again somewhat weaker than

AMTD
3, 1707–1742, 2010

Oxford's data.

Although there are indications for an annual cycle in MIPAS2-D data, neither sign nor distribution of patterns of differences do generally coincide with that of 1-D data. On average the values of the differences, either absolute or relative, are much lower than in 1-D data.

3.2.2 HNO_3

Figure 3 shows the same type of plots as in Fig. 1 for ESA and MIPAS2-D HNO_3 data. Again a conspicuous annual cycle can be seen in 1-D data, albeit the vertical structure of the difference profiles is distinct from that of CFC-11, in that there is a change of sign of the differences with altitude. The greatest absolute and relative differences are located at altitude regions where HNO_3 is rapidly varying with altitude. The sign of the differences at altitudes where the vmr decreases with height is consistent with the behavior of CFC-11 (mean values constant or decreasing with altitude). Relative differences of up to 20% may occur where HNO_3 values are still greater than half of the peak value.

Below 10 hPa there is only a seemingly random pattern visible in MIPAS2-D data.

In Fig. 4 latitude versus time plots at 80 hPa and at 12 hPa (i.e. at pressure levels where HNO_3 is increasing and decreasing with altitude, respectively) are shown for ESA HNO_3 data, as well as for MIPAS2-D data at 82 hPa and at 11 hPa. For middle and high latitudes 1-D data at 80 hPa features a similar pattern, albeit with opposite sign, as CFC-11 in the absolute differences. The sharp jump of the sign of the relative differences is due to extremely low HNO_3 volume mixing ratios around the equator. The time/latitude pattern of differences at a higher altitude (12 hPa) shows the same sign of the differences as the corresponding CFC-11 plot (Fig. 2). So again in both hemispheres, the sign of the differences in 1-D data essentially is the same for a given time and altitude.

MIPAS2-D absolute differences at the 82 hPa level show some distinct features, but again there is virtually no coincidence with those of 1-D data. At 11 hPa the picture is

AMTD
3, 1707–1742, 2010

not much different: a clear annual cycle is missing and coherent patches of the same sign in both hemispheres, as seen in 1-D data, are absent.

3.2.3 H_2O

Figure 5 gives a view on the behaviour of ESA and MIPAS2-D water vapour. At and below 200 hPa there is a clear annual cycle in 1-D data with the phase as in CFC-11, with the extremal relative differences reaching more than 50%. A cycle with reversed phase and maximum amplitude of 20% is discernible at altitudes around 120 hPa. The pressure level of approximately 160 hPa which divides the two phase regimes is close to the level of minimum water vapour vmr (left plot). Altitude regions of very great vertical negative gradients, essentially those below the tropopause, exhibit very high differences compared to the other species discussed so far. Again, the sign of the differences directly depends on the sign of the vertical vmr gradient. The cross section at pressure level 120 hPa (Fig. 6) shows in 1-D data a pattern which correlates partly with that of HNO_3 at 80 hPa, but is not very clear.

No features which hint at an annual cycle can be seen in 2-D data.

3.2.4 CFC-12, CH_4, N_2O

Beyond the species presented already, several more are processed by the diverse MIPAS L2 processors and a selection of these was analyzed with the same method. In Fig. 7 the features of mean vmr values and relative differences of CFC-12, CH_4, N_2O of Oxford 1-D and Bologna MIPAS2-D in the latitude bin 60° S–45° S are shown.

CFC-12

As already noted by Höpfner et al. (2007) there is also an effect in an old data version of IMK/IAA CFC-12 (Fig. 7 shows Oxford data due to better coverage). The overall picture is much like in CFC-11 of Oxford. Differences are pronounced in the altitude

region below 10 hPa. Again the maximum relative differences reach ±20% below the level of approximately half of the ground vmr value (at 40 hPa), while MIPAS2-D data does not show any clear pattern.

CH_4

Up to approximately 30 hPa there is a clear annual cycle with the relative difference amplitude reaching 15%. The phase of this cycle is consistent with that of CFC-11 up to 10 hPa. Above 10 hPa, at altitude levels where CH_4 vmr is still a quarter of the ground value, there is a reversal of the sign of the annual cycle. Again there are no noticeable features in MIPAS2-D data.

N_2O

A weak annual cycle, roughly consistent with CFC-11 is visible up to approximately 10 hPa. Maximum differences of 10–15% occur, but only for positive differences. MIPAS2-D relative differences depict no clear pattern below 10 hPa, while above the values are not reliable due to low volume mixing ratios and uncertainties comparable to the observed features.

4 Discussion

In the majority of the 1-D retrieval targets we analyzed, ascending/descending differences show a distinct annual cycle in the latitude range 60° S–45° S at pressure levels of 10–100 hPa, which roughly corresponds to 15–30 km altitude, i.e. to the lower stratosphere. Often an annual cycle is discernible in other latitudes too, with the sign of the differences at a given time of the year corresponding to that of the differences in 60° S–45° S at that time. Mostly no systematic features are visible in in 2-D retrieval data of the same species.

AMTD
3, 1707–1742, 2010

The relative lack of systematic features in the 2-D retrieval contrary to 1-D retrieval implies a connection of this anomaly to horizontal temperature gradients. Figure 8 shows the horizontal temperature gradient as seen along MIPAS' LOS. Since MIPAS is essentially looking backwards with respect to the platform's flight direction, the sign of the temperature gradient along LOS depends on whether the platform moves on the ascending or descending part of the orbit. In a region with temperature increasing northwards, MIPAS sees a negative gradient on ascending and a positve on descending movement, see e.g. the latitude −60° in the upper panel of the figure. The curves superimposed to the gradient field represent MIPAS' LOS for tangent altitudes 15, 20, and 25 km, the altitude region where most targets discussed in the preceding sections show a distinct annual cycle. The signs of the temperature gradients along LOS for latitudes with pronounced relative vmr differences (see e.g. Fig. 2), e.g. at 60° S or at 45° N for JJA months, or 45° S and 70° N for DJF months, respectively exhibit the same signs on ascending and descending orbit parts. The reversal of the gradient at 60° S for JJA months might partly explain the reversal of the sign in the annual cycle of CH_4 differences. From Fig. 9 it becomes clear that in the latitude band 60° S–45° S the horizontal gradient along constant latitude at altitudes corresponding to 10–100 hPa shows a periodic pattern over the course of the year with extremal values in DJF and JJA months.

Therefore, if there were a bias in the temperature/vmr retrievals due to a systematic error introduced by neglecting the effects of the temperature gradient, the annual cycle in the differences between ascending and descending orbit parts, as well as the global pattern of differences, would be explained in a natural way.

It has been noted already that for a given latitude band, signs of the ascending/descending differences seem to depend on the sign of the vmr profile's vertical gradient. This could be interpreted as vertical shift between the mean profiles of ascending and descending orbit parts. A vertical shift in turn would hint at a problem in the assignment of pressure in the ESA and Oxford retrievals and of the LOS in IMK/IAA retrievals. In all 1-D retrievals the pressure/LOS is jointly retrieved with the temperature.

This retrieved 1-D temperature profile is assumed to represent the whole 2-D temperature field for the gas retrievals along the instrument's LOS. Therefore it suggests itself to have a look into the temperature retrieval for the cause of the differences.

A set of four orbits (see Fig. 10) was processed with the IMK/IAA L2 processor, using a modified setup. This modified setup consists of the inclusion of an adequate horizontal temperature gradient in the forward modelling of the radiance spectrum during the temperature and LOS retrieval. The temperature gradient is calculated by finite differences on a grid of width 1° from ECMWF reanalysis temperature data (ERA-Interim) at each actual time/location of MIPAS measurements. The horizontal extension of the region influenced by the non-zero temperature gradient was assumed to be 400 km. The subsequent species retrievals then were fed with the temperature profile and LOS information of this modified first step in the retrieval chain. No other changes in the retrieval of the species were made.

The data set comprises two orbit pairs: 4482, 4489, and 4483, 4490 of 8 January 2003. The orbits were chosen pairwise such that in the latitude range 60° S–45° S the geolocations have approximately the same longitude values, as it can be seen in Fig. 10. The key difference of orbits of a pair is that MIPAS scans the region on an ascending orbit part for the one and on a descending part for the other one, with a time lag of approximately 12 h. In what follows we shall call the area at 60° S–45° S/115° W region W and at 60° S–45° S/65°E the region E.

Figure 11 shows the temperature field T along the orbit and differences in the temperature field caused by the inclusion of the horizontal temperature gradient. The difference is calculated as T of data of the modified setup minus T of data version V3O_T_8. Obviously, values of differences are high where the horizontal temperature gradient is most pronounced. This is the case for the latitude region 45° S–60° S as well as in the vicinity of the winter pole (northern polar vortex). At altitudes up to roughly 100 hPa the differences reach ±3 K, while above ±1–2 K are found. It is essential that although the difference plots for the two orbits look quite similar, there is a major difference in that the signs of the differences are opposite for each of the regions E and W (notice the

AMTD
3, 1707–1742, 2010

reversal of the relative position of E and W in the two orbits).

In Fig. 12 the resulting absolute vmr differences of CFC-11 and HNO_3 are presented. Differences are calculated between vmr of the retrievals fed with the changed temperature and LOS data, and vmr of data versions V3O_F-11_8 and V3O_HNO3_7. Again the signs of the differences for each of the regions E and W only depend on whether the corresponding measurements were taken on an ascending or descending orbit part. Therefore in a difference of means of profiles of ascending orbit parts (W for orbit 4483, E for 4490) and means of profiles of descending orbit parts (E for 4483,W for 4490) the contributions will not cancel out but rather approximately double the value of a single difference.

A condensed presentation of the differences between the results of the modified processing and the old data is given in Fig. 13 for data of all four orbits. There is a conspicuous impact of the modification of the IMK/IAA L2 processor on the temperature profiles. In the pressure range 10–300 hPa there is a clear decrease of the absolute differences. Ascending/descending differences around the 100 hPa level even change from −5 K to −1 K. Obviously these changes in the temperatures by entering the retrieval of CFC-11 have a significant positive impact on the CFC-11 absolute differences. For the V3O_F-11_8 data the absolute differences are in good agreement with the January 2003 values of Fig. 1, while CFC-11 ascending/descending differences of the modified L2 processing are much closer to zero. The improvement can well be seen in the relative differences. In HNO_3 there is an advantage of data of the modified processing over V3O_HNO3_7 data only above 30 hPa.

Altogether this means that already the inclusion of an appropriate external horizontal temperature gradient in a 1-D retrieval attenuates the ascending/descending differences.

This does not imply that the temperature field inhomogeneities are the only cause for deviations of 1-D retrieved vmr profiles from true atmospheric state, as it is known that inhomogeneities in the species vmr fields might well cause significant deviations too (Swartz et al., 2006). However, for mid IR limb sounding the temperature profile is a

AMTD
3, 1707–1742, 2010

key quantity with strong influence on all species retrievals, which makes it so important to know this quantity as accurate as possible.

5 Conclusions

To sum up our conclusions with respect to the phenomenon's cause, impact and implications:

1. For several species there is a difference in 1-D retrieval species' profiles between ascending and descending parts of the orbit, which is not explainable in terms of chemistry or dynamics. For some species monthly means of relative differences in certain regions can reach 20% in the lower stratosphere.
2. Data from a 2-D retrieval do not show a corresponding systematic behaviour.
3. The pattern of the differences with respect to altitude and latitude implies that there is a combined effect of temperature gradient along MIPAS' LOS – which, for the same meridional temperature gradient, changes sign between ascending and descending orbit parts – and the species' vertical gradient.
4. A simple correction strategy, namely the inclusion of externally given horizontal temperature gradients in the forward calculations of the 1-D retrievals, appropriate for time and location of the measurements, significantly reduces the ascending/descending differences for a test data set of four orbits.

There are two options to deal with the problem:

1. Passive approach: for data of 1-D processors a thorough error characterization including effects of temperature field inhomogeneities will be necessary.
2. Active approach: data processing should be carried out with processors capable of fully handling inhomogeneities (such as the GMTR, Carlotti et al., 2006) or

AMTD
3, 1707–1742, 2010

at least those of the temperature field in the atmosphere (such as the gradient inclusion strategy employed in this study).

Implications for the users of MIPAS data of 1-D L2 processors are:

1. In any work using profiles of MIPAS 1-D retrievals it has to be checked whether the phenomenon demonstrated in this paper has to be taken into account.

2. Especially validation work should be very carefully designed to avoid a bias due to the 1-D processor induced asymmetry of data of ascending and descending orbit parts.

3. Averages of 1-D data should best be calculated by first averaging profiles of ascending and descending orbit parts separately and averaging the two average profiles then. The latter average has to be performed without weighting by the number of profiles which entered the ascending/descending averages.

4. Since we have found differences of a certain extent in monthly means, we can not exclude that single profiles, or even averages of few profiles, will show deviations from the true atmosphere which are larger than that extent.

One must be aware that 1-D retrieval from measurements of other infrared limb emission sounders might also be affected by the effects described here if there are temperature gradients along the LOS. The same conclusions as above are likely to hold for these instruments with respect to their 1-D L2 processors too.

Acknowledgements. Enrico Arnone acknowledges funding through the European Community's Human Potential Programme Marie Curie under contract MERG-CT-2007-209157. Enzo Papandrea acknowledges support by ESA within the framework of the Changing Earth Science Network Initiative. Fabrizio Niro (Serco) and Thorsten Fehr (ESA/ESRIN) have provided data and documents. The retrievals of IMK/IAA were performed partly on the HP XC4000 of the Scientific Supercomputing Center (SSC) Karlsruhe under project grant MIPAS.

References

Bernath, P.: Atmospheric Chemistry Experiment, in Optical Remote Sensing of the Atmosphere, OSA Technical Digest, Optical Society of America, Washington, DC, p. 22, 1999. 1710

Bernath, P. F., McElroy, C. T., Abrams, M. C., Boone, C. D., Butler, M., Camy-Peyret, C., Carleer, M., Clerbaux, C., Coheur, P.-F., Colin, R., DeCola, P., De Mazière, M., Drummond, J. R., Dufour, D., Evans, W. F. J., Fast, H., Fussen, D., Gilbert, K., Jennings, D. E., Llewellyn, E. J., Lowe, R. P., Mahieu, E., McConnell, J. C., McHugh, M., McLeod, S. D., Michaud, R., Midwinter, C., Nassar, R., Nichitiu, F., Nowlan, C., Rinsland, C. P., Rochon, Y. J., Rowlands, N., Semeniuk, K., Simon, P., Skelton, R., Sloan, J. J., Soucy, M.-A., Strong, K., Tremblay, P., Turnbull, D., Walker, K. A., Walkty, I., Wardle, D. A., Wehrle, V., Zander, R., and Zou, J.: Atmospheric Chemistry Experiment (ACE): Mission overview, Geophys. Res. Lett., 32(15), L15S01, doi:10.1029/2005GL022386, 2005. 1710

Carlotti, M.: Global-fit approach to the analysis of limb–scanning atmospheric measurements, Appl. Optics, 27, 3250–3254, 1988. 1712

Carlotti, M., Dinelli, B. M., Raspollini, P., and Ridolfi, M.: Geo-fit approach to the analysis of limb–scanning satellite measurements, Appl. Optics, 40, 1872–1885, 2001. 1709, 1710, 1711, 1714

Carlotti, M., Brizzi, G., Papandrea, E., Prevedelli, M., Ridolfi, M., Dinelli, B. M., and Magnani, L.: GMTR: Two–dimensional geo–fit multitarget retrieval model for Michelson Interferometer for Passive Atmospheric Sounding/ Environmental Satellite observations, Appl. Optics, 45, 716–727, 2006. 1710, 1714, 1724

Carlotti, M., Dinelli, B. M., Papandrea, E., and Ridolfi, M.: Assessment of the horizontal resolution of retrieval products derived from MIPAS observations, Opt. Express, 15, 10458–10472, 2007. 1715

Dinelli, B. M., Alpaslan, D., Carlotti, M., Magnani, L., and Ridolfi, M.: Multi–target retrieval (MTR): the simultaneous retrieval of pressure, temperature and volume mixing ratio profiles from limb–scanning atmospheric measurements, J. Quant. Spectrosc. Ra., 84, 141–157, 2004. 1714

Dinelli, B. M., Arnone, E., Brizzi, G., Carlotti, M., Castelli, E., Magnani, L., Papandrea, E., Prevedelli, M., and Ridolfi, M.: The MIPAS2D database of MIPAS/ENVISAT measurements retrieved with a multi-target 2-dimensional tomographic approach, Atmos. Meas. Tech., 3,

355–374, 2010,
http://www.atmos-meas-tech.net/3/355/2010/. 1714
Dudhia, A., Jay, V. L., and Rodgers, C. D.: Microwindow selection for high–spectral–resolution sounders, Appl. Optics, 41, 3665–3673, 2002. 1711
Fischer, H., Blom, C., Oelhaf, H., Carli, B., Carlotti, M., Delbouille, L., Ehhalt, D., Flaud, J.-M., Isaksen, I., López-Puertas, M., McElroy, C. T., and Zander, R.: Envisat-MIPAS, an instrument for atmospheric chemistry and climate research, European Space Agency-Report SP-1229, C. Readings and R. A. Harris (eds.), ESA Publications Division, ESTEC, P. O. Box 299, 2200 AG Noordwijk, The Netherlands, 2000. 1709
Fischer, H., Birk, M., Blom, C., Carli, B., Carlotti, M., von Clarmann, T., Delbouille, L., Dudhia, A., Ehhalt, D., Endemann, M., Flaud, J. M., Gessner, R., Kleinert, A., Koopman, R., Langen, J., López-Puertas, M., Mosner, P., Nett, H., Oelhaf, H., Perron, G., Remedios, J., Ridolfi, M., Stiller, G., and Zander, R.: MIPAS: an instrument for atmospheric and climate research, Atmos. Chem. Phys., 8, 2151–2188, 2008,
http://www.atmos-chem-phys.net/8/2151/2008/. 1709
Funke, B., López-Puertas, M., García-Comas, M., Stiller, G. P., von Clarmann, T., Höpfner, M., Glatthor, N., Grabowski, U., Kellmann, S., and Linden, A.: Carbon monoxide distributions from the upper troposphere to the mesosphere inferred from 4.7 µm non-local thermal equilibrium emissions measured by MIPAS on Envisat, Atmos. Chem. Phys., 9, 2387–2411, 2009,
http://www.atmos-chem-phys.net/9/2387/2009/. 1714
Höpfner, M., von Clarmann, T., Engelhardt, M., Fischer, H., Funke, B., Glatthor, N., Grabowski, U., Kellmann, S., Kiefer, M., Linden, A., López-Puertas, M., Milz, M., Steck, T., Stiller, G. P., Wang, D. Y., Ruhnke, R., Kouker, W., Reddmann, T., Bernath, P., Boone, C., and Walker, K. A.: Comparison between ACE-FTS and MIPAS IMK/IAA profiles of O_3, H_2O, N_2O, CH_4, CFC-11, CFC-12, HNO_3, $ClONO_2$, NO_2, N_2O_5, CO, and SF_6 in February/March 2006, in Proc. Third Workshop on the Atmospheric Chemistry Validation of Envisat, (ACVE-3), 4–7 December, 2006, ESRIN, Frascati, Italy, vol. ESA SP–642, CD-ROM, ESA Publications Division, ESTEC, Postbus 299, 2200 AG Noordwijk, The Netherlands, 2007. 1710, 1716, 1719
Kleinert, A., Aubertin, G., Perron, G., Birk, M., Wagner, G., Hase, F., Nett, H., and Poulin, R.: MIPAS Level 1B algorithms overview: operational processing and characterization, Atmos. Chem. Phys., 7, 1395–1406, 2007,

http://www.atmos-chem-phys.net/7/1395/2007/. 1711
Livesey, N. J. and Read, W. G.: Direct retrieval of line–of–sight atmospheric structure from limb sounding observations, Geophys. Res. Lett., 27, 891–894, 2000. 1710
Papandrea, E., Arnone, E., Brizzi, G., Carlotti, M., Castelli, E., Dinelli, B. M., and Ridolfi, M.: Two-dimensional tomographic retrieval of MIPAS/ENVISAT measurements of ozone and related species, Int. J. Remote Sens., 31, 477–483, 2010. 1714
Raspollini, P., Belotti, C., Burgess, A., Carli, B., Carlotti, M., Ceccherini, S., Dinelli, B. M., Dudhia, A., Flaud, J.-M., Funke, B., Hpfner, M., Lpez-Puertas, M., Payne, V., Piccolo, C., Remedios, J. J., Ridolfi, M., and Spang, R.: MIPAS level 2 operational analysis, Atmos. Chem. Phys., 6, 5605–5630, 2006, http://www.atmos-chem-phys.net/6/5605/2006/. 1712
Remedios, J. J., Leigh, R. J., Waterfall, A. M., Moore, D. P., Sembhi, H., Parkes, I., Greenhough, J., Chipperfield, M. P., and Hauglustaine, D.: MIPAS reference atmospheres and comparisons to V4.61/V4.62 MIPAS level 2 geophysical data sets, Atmos. Chem. Phys. Discuss., 7, 9973–10017, 2007, http://www.atmos-chem-phys-discuss.net/7/9973/2007/. 1713
Rodgers, C. D.: Inverse Methods for Atmospheric Sounding: Theory and Practice, vol. 2 of Series on Atmospheric, Oceanic and Planetary Physics, F. W. Taylor, ed., World Scientific, 2000. 1712, 1714
Steck, T., Höpfner, M., von Clarmann, T., and Grabowski, U.: Tomographic retrieval of atmospheric parameters from infrared limb emission observations, Appl. Optics, 44, 3291–3301, 2005. 1710, 1711
Swartz, W. H., Yee, J.-H., Randall, C. E., Shetter, R. E., Browell, E. V., Burris, J. F., McGee, T. J., and Avery, M. A.: Comparison of high-latitude line-of-sight ozone column density with derived ozone fields and the effects of horizontal inhomogeneity, Atmos. Chem. Phys., 6, 1843–1852, 2006, http://www.atmos-chem-phys.net/6/1843/2006/. 1723
von Clarmann, T. and Echle, G.: Selection of optimized microwindows for atmospheric spectroscopy, Appl. Optics, 37, 7661–7669, 1998. 1711
von Clarmann, T., Glatthor, N., Grabowski, U., Höpfner, M., Kellmann, S., Kiefer, M., Linden, A., Mengistu Tsidu, G., Milz, M., Steck, T., Stiller, G. P., Wang, D. Y., Fischer, H., Funke, B., Gil-López, S., and López-Puertas, M.: Retrieval of temperature and tangent altitude pointing from limb emission spectra recorded from space by the Michelson Inter-

ferometer for Passive Atmospheric Sounding (MIPAS), J. Geophys. Res., 108(D23), 4736, doi:10.1029/2003JD003602, 2003. 1713

von Clarmann, T., Höpfner, M., Kellmann, S., Linden, A., Chauhan, S., Funke, B., Grabowski, U., Glatthor, N., Kiefer, M., Schieferdecker, T., Stiller, G. P., and Versick, S.: Retrieval of temperature, H_2O, O_3, HNO_3, CH_4, N_2O, $ClONO_2$ and ClO from MIPAS reduced resolution nominal mode limb emission measurements, Atmos. Meas. Tech., 2, 159–175, 2009, http://www.atmos-meas-tech.net/2/159/2009/. 1714

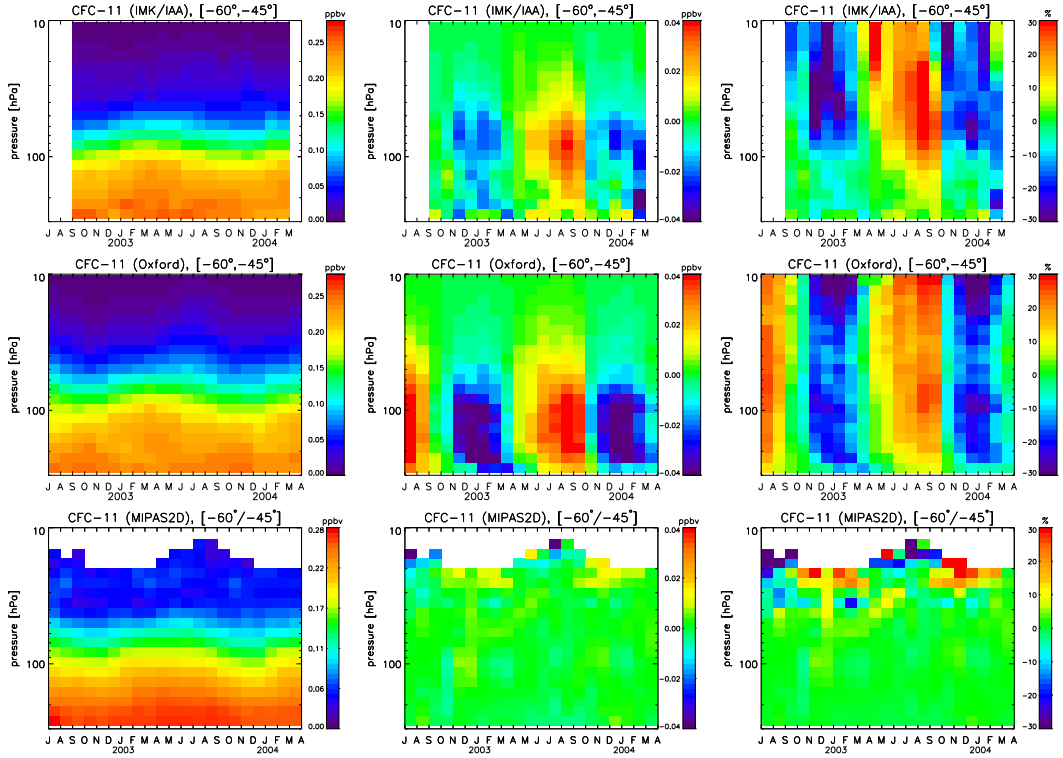

Fig. 1. Distribution of average values of CFC-11 (left column), of ascending/descending differences (middle column), and relative differences (right) for 1-D retrievals (top row: IMK/IAA, middle row: Oxford) and for 2-D retrievals (MIPAS2-D, bottom row). Time bin is one month, latitude bin is 60° S to 45° S. Altitude bins for 1-D and 2-D data are explained in Sect. 3.1. The tick marks of the time axis give the begin of the months and years, respectively.

AMTD
3, 1707–1742, 2010

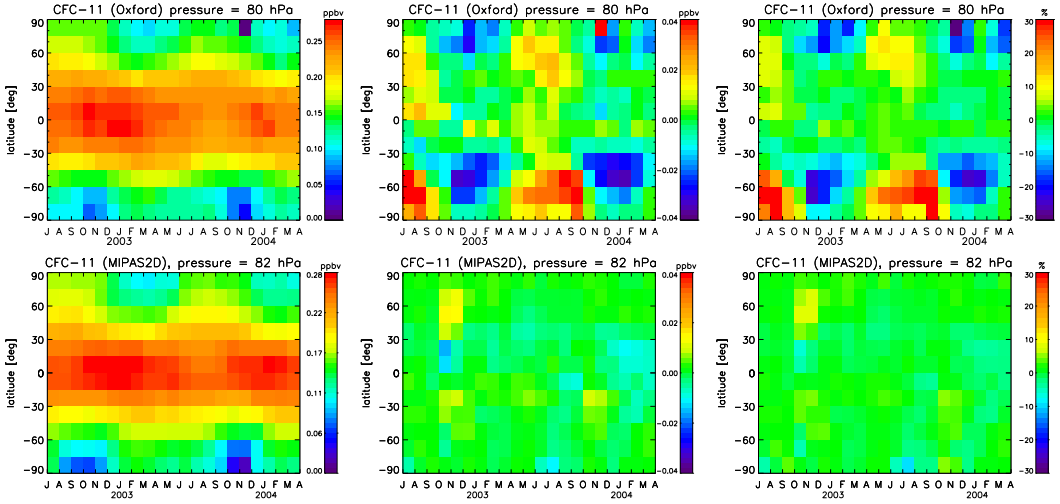

Fig. 2. Distribution of mean values of CFC-11 vmr (left column), ascending/descending differences (middle column), and relative differences (right) for Oxford 1-D (top row) and Bologna MIPAS2-D (bottom row) retrievals. Time bin is one month, latitude bin is 15°, pressure is 80 hPa for Oxford and 82 hPa for MIPAS2-D data.

AMTD
3, 1707–1742, 2010

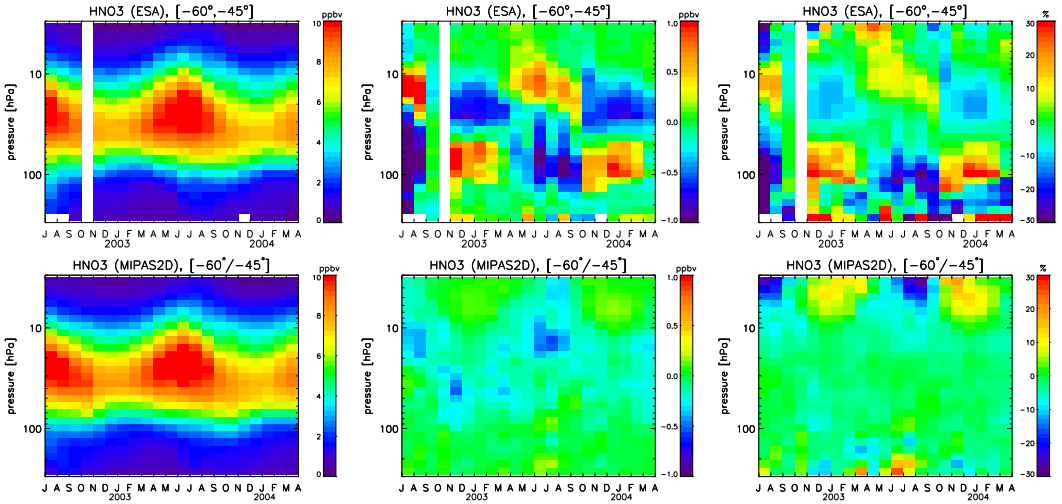

Fig. 3. Same as Fig. 1, but for HNO_3 of ESA 1-D (top) and MIPAS2-D (bottom) retrievals.

AMTD
3, 1707–1742, 2010

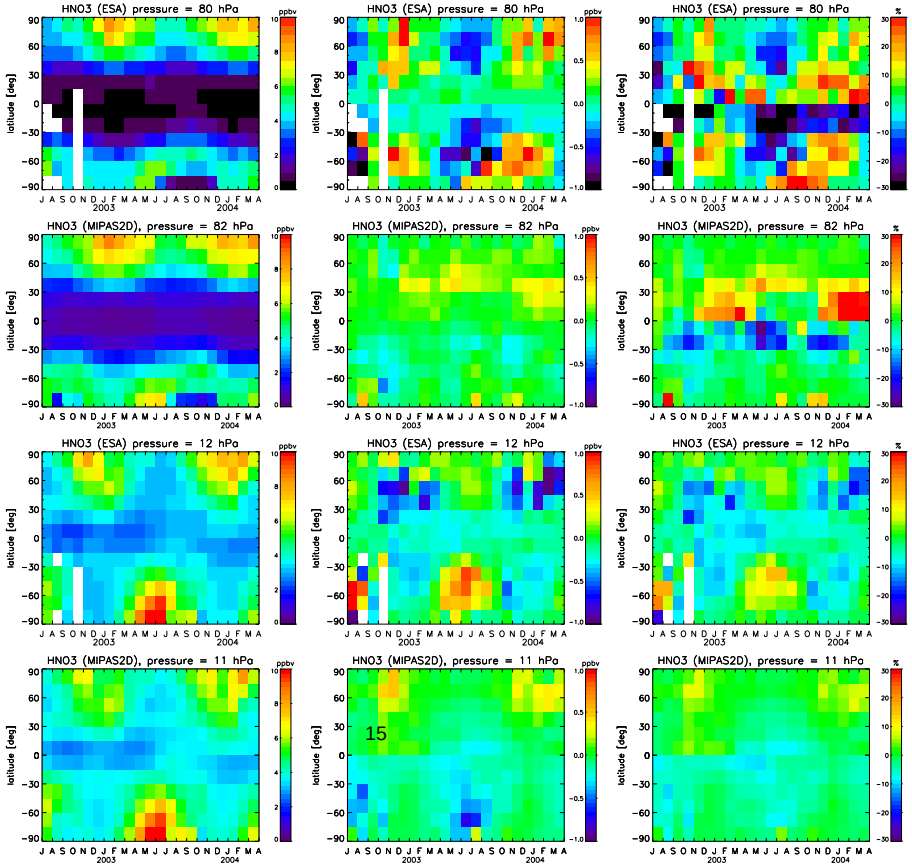

Fig. 4. Distribution of average HNO_3 (left column), ascending/descending differences (middle), and relative differences (right) for ESA 1-D data at 80 hPa (first row), MIPAS2-D at 82 hPa (second), ESA 1-D at 12 hPa (third), and MIPAS2-D at 11 hPa (last). Data bins are the same as in Fig. 2.

AMTD
3, 1707–1742, 2010

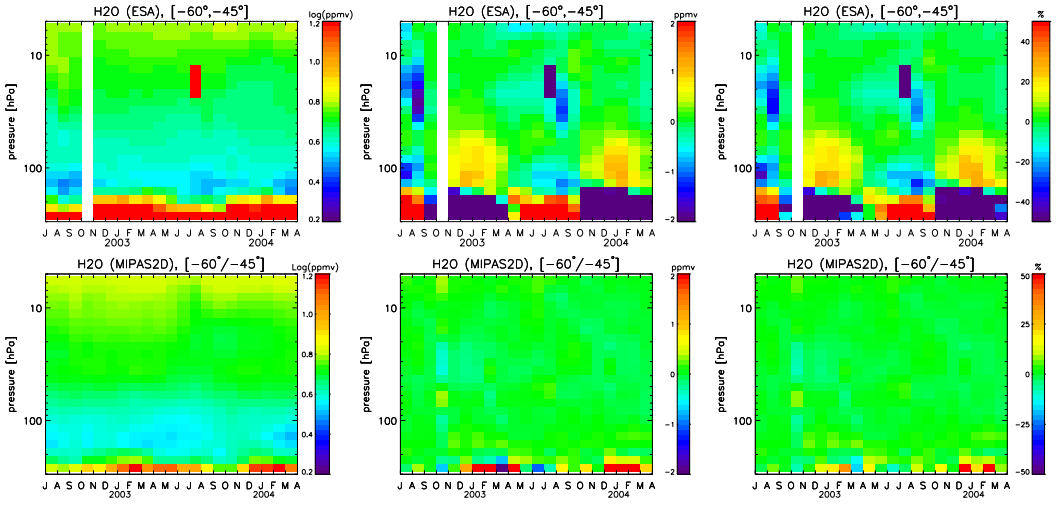

Fig. 5. As Fig. 1, but for ESA (top) and Bologna MIPAS2-D (bottom) L2 data of H_2O. Note that the plot of the average data has a logarithmic scaling of the values, while absolute and relative differences have a linear one and that the scale of the relative errors is larger (±50%) than with the other species shown.

AMTD
3, 1707–1742, 2010

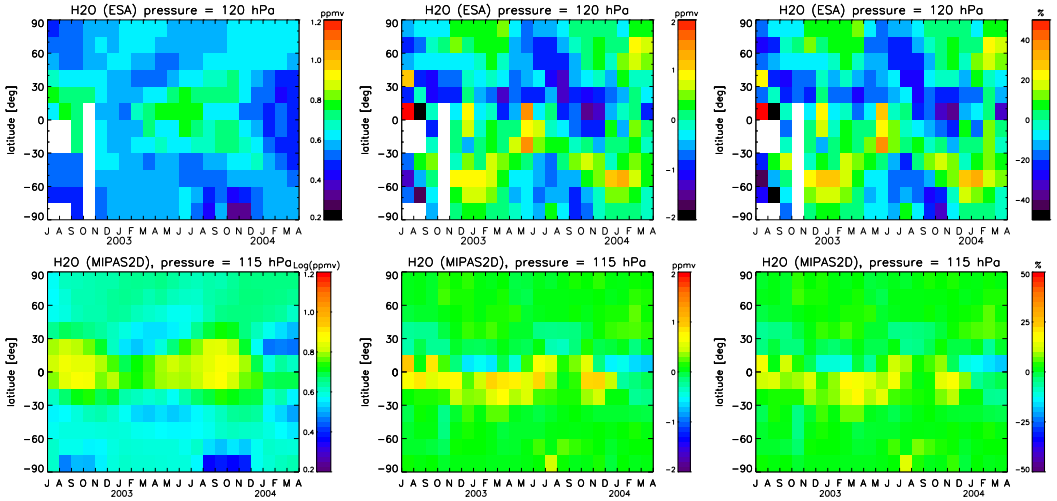

Fig. 6. As Fig. 2, but water vapour for ESA data at 120 hPa (top row) and MIPAS2-D data at 115 hPa (bottom).

AMTD
3, 1707–1742, 2010

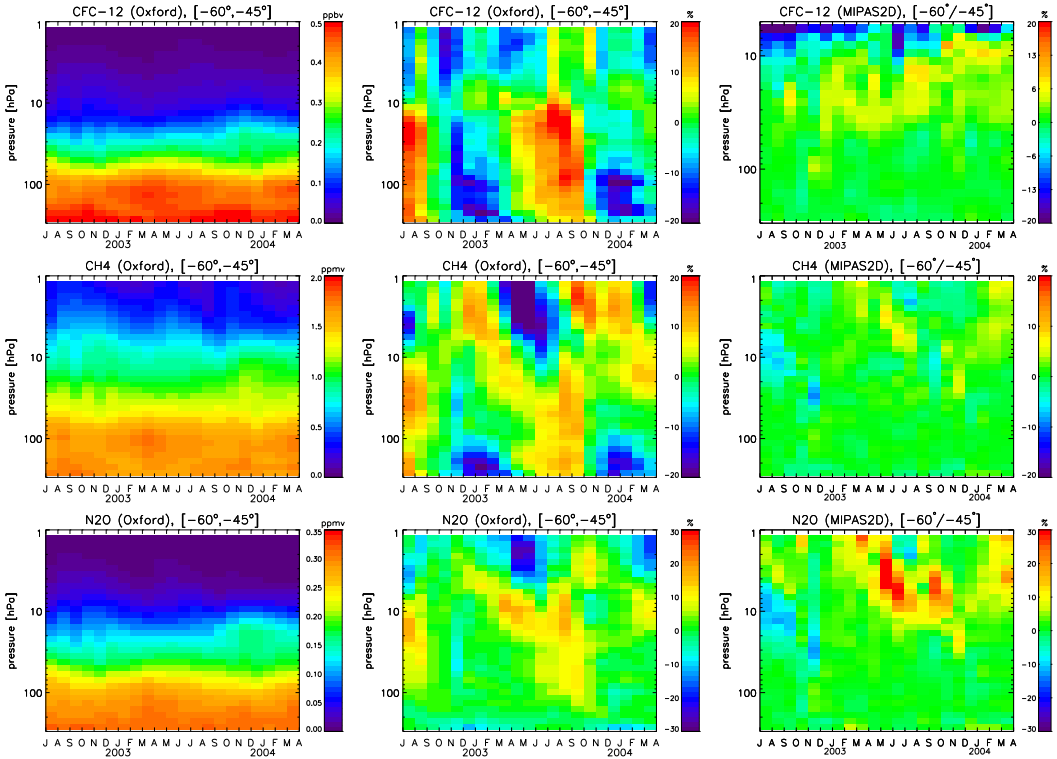

Fig. 7. Absolute values of Oxford (left column) and relative differences for Oxford (middle column) and Bologna MIPAS2-D (right column) of CFC-12, CH_4, and N_2O (top to bottom row, respectively) in the latitude bin 60° S–45° S.

AMTD
3, 1707–1742, 2010

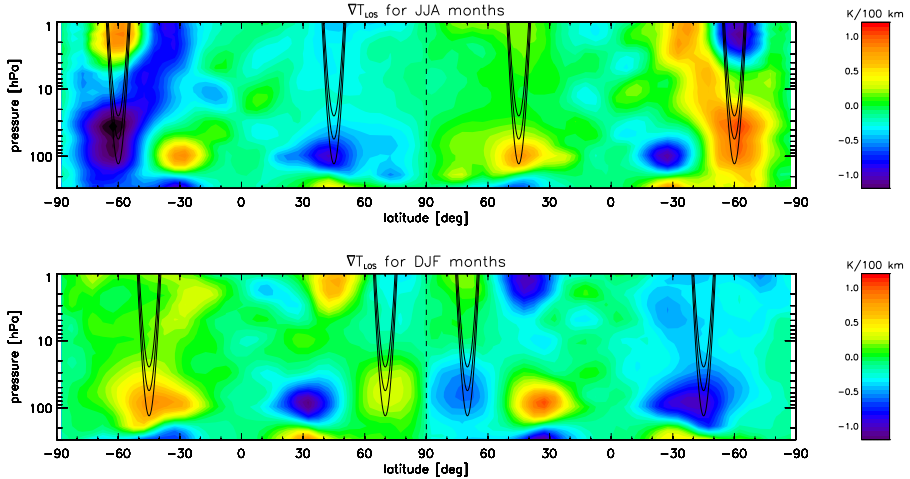

Fig. 8. Horizontal temperature gradient along MIPAS' LOS averaged for JJA (top) and DJF months. The gradient is calculated from ECMWF reanalysis temperature fields. The latitude coordinate begins at the South Pole on the left side, first follows the ascending part of an orbit up to the North Pole (broken line at 90°), and then follows the descending orbit part down to the South Pole again. Superimposed curves represent MIPAS' LOS for tangent altitudes 15, 20, and 25 km for measurement locations at 60° S and 45° N (top panel) and 45° S and 70° N (bottom).

AMTD
3, 1707–1742, 2010

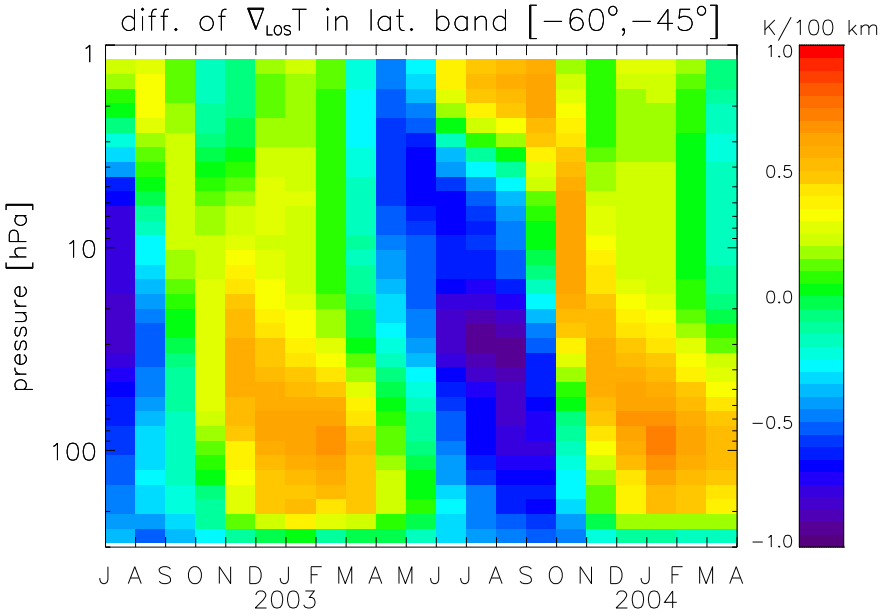

Fig. 9. Differences of horizontal temperature gradients along MIPAS' LOS between ascending and descending orbit parts. Temperature data was taken from ECMWF reanalysis data on MIPAS measurement geolocations, and the method presented in Sect. 3.1 was applied.

AMTD
3, 1707–1742, 2010

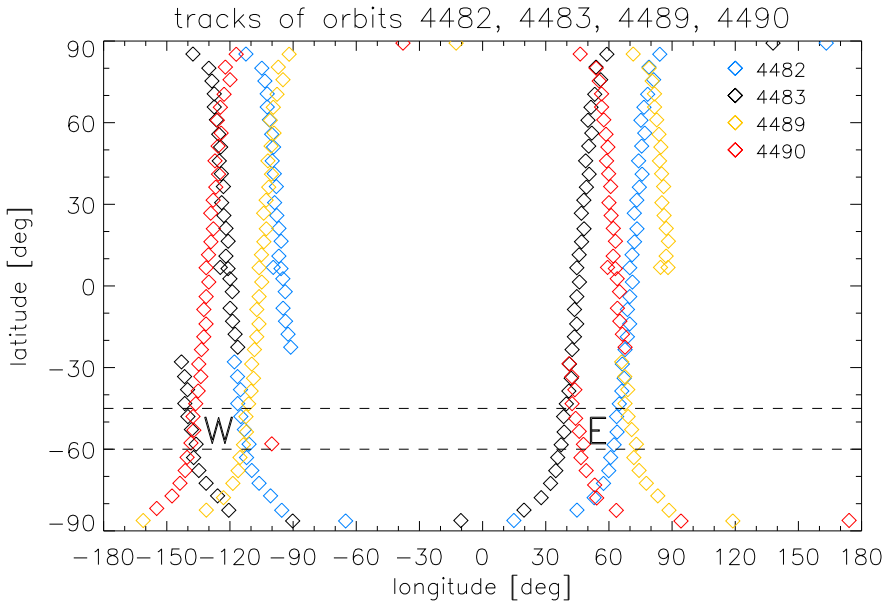

Fig. 10. Geolocations of the four orbits selected to test the influence of the inclusion of an external temperature gradient in the forward model of the 1-D retrieval. Ascending parts of the orbits feature an inclination to the left while descending orbit parts are inclined to the right.

AMTD
3, 1707–1742, 2010

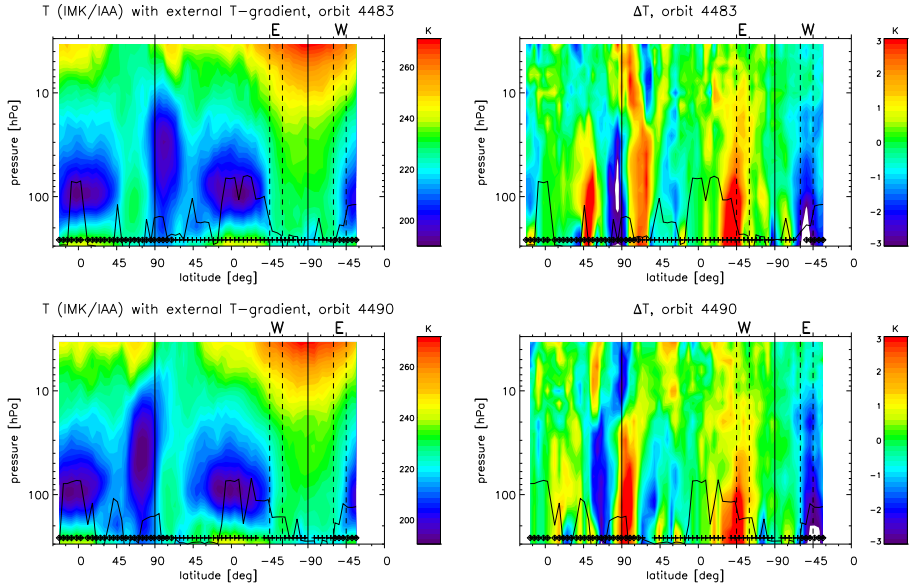

Fig. 11. Temperature field (left column) along orbits 4483 (top row) and 4490 (bottom) as retrieved with the modified IMK/IAA L2 data processor (details see text). The orbit starts at the plot frame's left side at approximately 20° S. The right column gives the differences in the temperature fields along the respective orbits. Differences are calculated per geolocation as T of modified retrieval minus T of 1-D IMK/IAA data (version V3O_T_8). Vertical lines indicate the latitude band 45° S–60° S (dashed) and the poles (−90 is the South Pole). The continuous line running between the frames' lower boundary and 60 hPa indicates the pressure level of the lowest tangent altitudes used in the retrievals. Near the bottom of the plot frame plus signs indicate measurements with and diamonds measurements without daylight. Capitals W and E above the plot frames indicate the longitude regions 115° W and 65° E, respectively (see Fig. 10 and text).

AMTD
3, 1707–1742, 2010

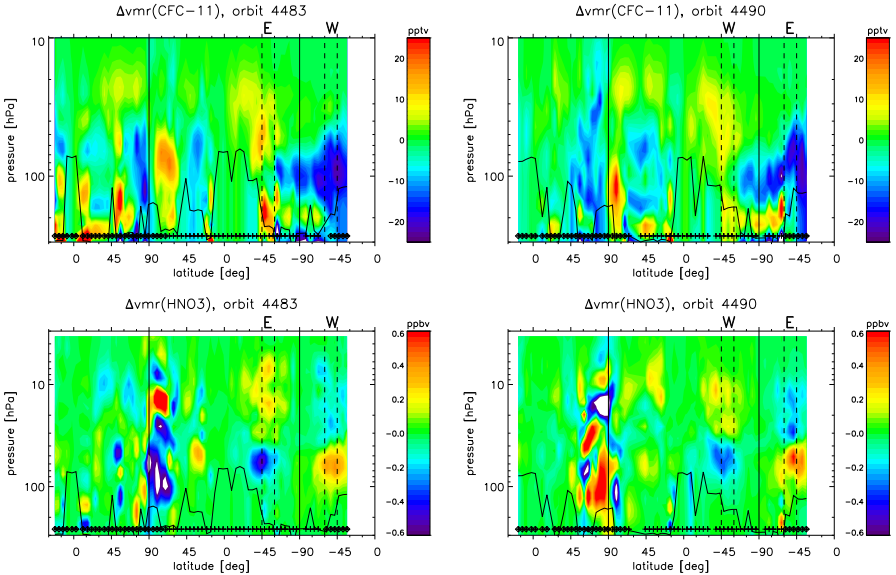

Fig. 12. Absolute differences between retrieval data of modified and original 1-D processing for vmr of CFC-11 (top row) and HNO_3 for orbits 4483 (left column) and 4490. Meaning of vertical and other lines and symbols as in Fig. 11.

AMTD
3, 1707–1742, 2010

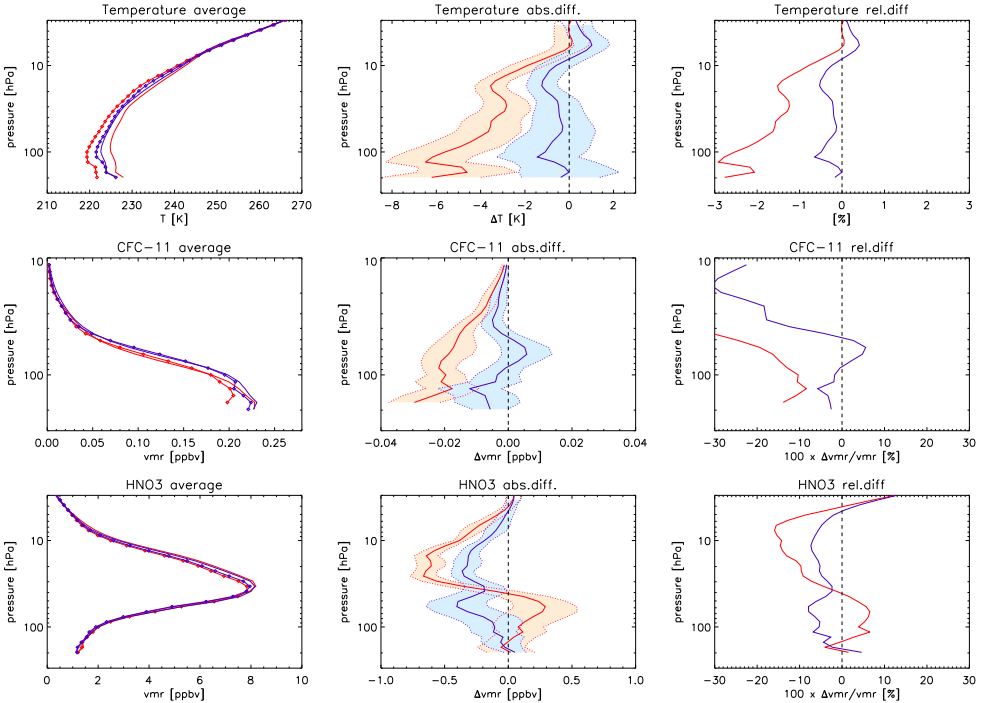

Fig. 13. Compilation in the latitude band 60° S–45° S of the differences between data of ascending and descending orbit parts for the old IMK/IAA data (red curves) and for the data from the modified IMK/IAA processor (blue). Averages over orbits 4482, 4483, 4489, and 4490 are shown in the left column for temperature (top row), CFC-11 (middle), and HNO_3 (bottom); data is separately averaged for ascending (solid line) and descending (solid line with symbols) orbit parts. Absolute differences between ascending and descending data are shown in the middle, relative differences are presented in the right column.

AMTD
3, 1707–1742, 2010